

## Article

# Chromite Mineralization in the Sopcheozero Deposit (Monchegorsk Layered Intrusion, Fennoscandian Shield)

Artem V. Mokrushin <sup>1,\*</sup> and Valery F. Smol'kin <sup>2</sup>

<sup>1</sup> Geological Institute—Subdivision of the Federal Research Centre “Kola Science Centre of the Russian Academy of Sciences”, 14 Fersman Street, 184209 Apatity, Russia

<sup>2</sup> Vernadsky State Geological Museum of the Russian Academy of Sciences, 11/11 Mokhovaya Street, 125009 Moscow, Russia; vsmolkin@sgm.ru

\* Correspondence: mokrushin@geoksc.apatity.ru; Tel.: +7-(902)133-39-95

**Abstract:** In 1990, the Sopcheozero Cr deposit was discovered in the Monchegorsk Paleoproterozoic layered mafic-ultramafic layered intrusion (Monchepluton). This stratiform early-magmatic deposit occurs in the middle part of the Dunite Block, which is a member of the Monchepluton layered series. The Cr<sub>2</sub>O<sub>3</sub> average-weighted content in ordinary and rich ores of the deposit is 16.65 and 38.76 wt.%, respectively, at gradually changing concentrations within the rich, ordinary and poor ore types and ore body in general. The ores of the Sopcheozero deposit, having a ratio of Cr<sub>2</sub>O<sub>3</sub>/FeO<sub>total</sub> = 0.9–1.7, can serve as raw materials for the refractory and chemical industries. The ore Cr-spinel (magnochromite and magnoaluminochromite) is associated with highly magnesian olivine (96–98 Fo) rich in Ni (0.4–1.1 wt.%). It confirms a low S content in the melt and complies with the low oxygen fugacity. The coexisting Cr-spinel-olivine pairs crystallized at temperatures from 1258 to 1163 °C, with accessory Cr-spinel crystallizing at relatively low, while ore Cr-spinel at higher temperatures. The host rock and ore distinguish with widespread plastic deformations of olivine at the postcrystallization phase under conditions of high temperature (above 400 °C) and pressure (5 kbar). At the post magmatic Svecofennian stage (1.84 Ga), the deposit, jointly with the Monchepluton, was subject to diverse tectonic deformations.

**Keywords:** Cr-spinel; layered mafic-ultramafic intrusion; Sopcheozero deposit; Monchepluton; Fennoscandian Shield; Russia



**Citation:** Mokrushin, A.V.; Smol'kin, V.F. Chromite Mineralization in the Sopcheozero Deposit (Monchegorsk Layered Intrusion, Fennoscandian Shield). *Minerals* **2021**, *11*, 772. <https://doi.org/10.3390/min11070772>

Academic Editors: Evgenii Pushkarev and Giorgio Garuti

Received: 9 May 2021  
Accepted: 14 July 2021  
Published: 16 July 2021

**Publisher's Note:** MDPI stays neutral with regard to jurisdictional claims in published maps and institutional affiliations.



**Copyright:** © 2021 by the authors. Licensee MDPI, Basel, Switzerland. This article is an open access article distributed under the terms and conditions of the Creative Commons Attribution (CC BY) license (<https://creativecommons.org/licenses/by/4.0/>).

## 1. Introduction

The largest chromite deposits are confined to the ophiolite formation and mafic-ultramafic layered intrusions. In the results of comprehensive studies of the layered intrusions of the Fennoscandian Shield, the Sopcheozero chromite deposit was discovered. In 1992, geologists of the Central Kola Expedition (V.V. Sholokhnyov and G.F. Bakayev) performed general exploration work in promising areas under the contract with the OJSC “Severonickel Combine”. In 1995–1996, exploration work showed that the deposit has 8.7 million tons of reserves and 12 million tons of resources with a cut-off Cr<sub>2</sub>O<sub>3</sub> content of 10 wt.% and an average ore grade of 23.1%. A total of 102 boreholes (17.9 ths running meters) were drilled within the Sopcheozero deposit, including 54 boreholes that penetrated the ore deposit. From 1998 to 2004, geological exploration was provided to study the geology and geochronology of deposit and the entire Monchepluton. The work was carried out jointly with geologists of the OJSC “Severonickel Combine”, Geological Institute KSC RAS, Mining Institute KSC RAS and Gipronickel Institute JSC (St. Petersburg) [1–3].

The aim of this study is to define the genesis of the Cr-spinel mineralization and to detect the location of the Dunite Block in the Monchepluton based on geological-structural, geochronological, petrological and mineralogical data on the Sopcheozero deposit obtained at complex geological prospecting by drilling. The quarry is currently filled with water and the primary ore body is unavailable for study. Later works dedicated to the ores of the

Sopchezero deposit [4,5] are based on samples from dumps (Figure 1) preserved at the bottom of Mt. Nittis.



**Figure 1.** Panorama of Mt. Nittis: (A)—(1) A quarry of the Sopchezero deposit and overburden dumps; (B)—(2) In 2015, the quarry was filled with water; (3) Large fragments of Cr-spinel ores and host dunites have been preserved on its terrace.

#### *Geological Background*

The Monchepluton is a typical 2.5 Ga layered intrusion containing deposits and prospects of chrome, sulfide Cu-Ni and PGE ores (Figures 2 and 3) [6–10]. According to the U-Pb zircon and baddeleyite analysis, the age of the Monchepluton rocks ranges within 2507–2493 Ma [1,11,12]. Using the U-Pb dating of zircon, age of the dunite has been defined as  $2500 \pm 10$  Ma, as well as  $2500 \pm 2$  Ma for the high-grade chromium ore [13]. The Monchepluton has distinct intrusive contacts with host rocks, which are represented by various Archean gneisses and amphibolites. The pluton's rocks are, in turn, overlain by conglomerates and weathering crust rocks in the Vurechuaivench foreland at the basement of the metavolcanic unit in the Strel'nya Series in the Imandra–Varzuga zone [14].

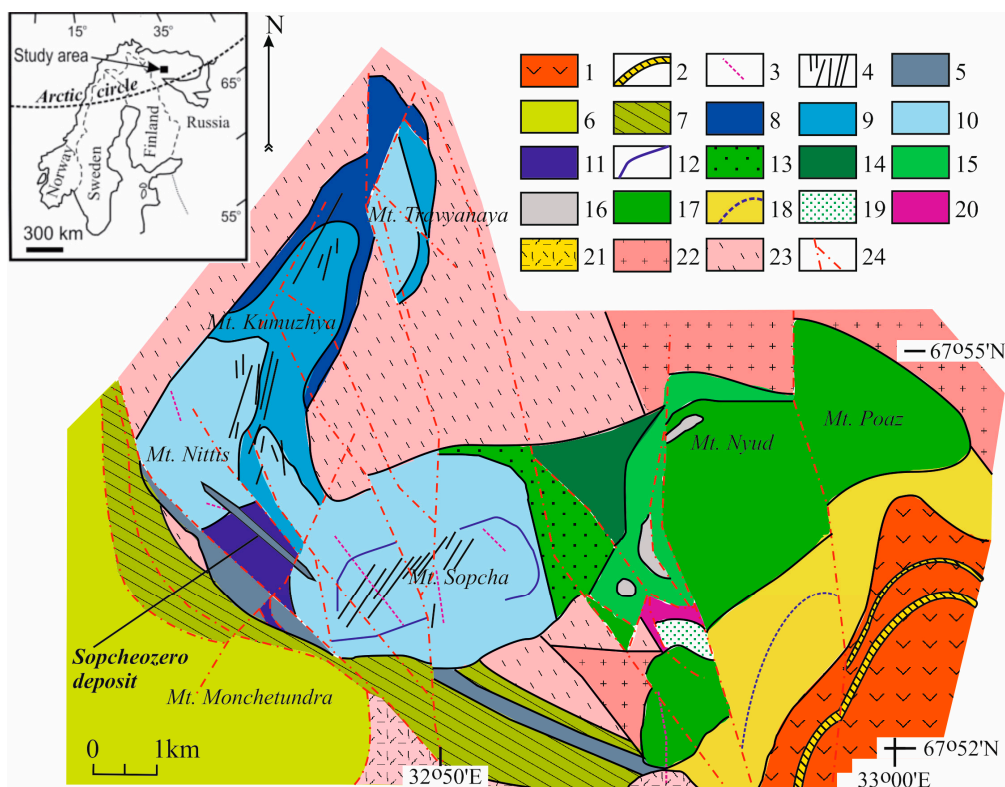


**Figure 2.** Geological map of the Monchepluton [1]. (1) Metavolcanics and (2) quartzite and schist of the Kuksha and Seidorechka formations of the Imandra–Varzuga Zone; (3) metadolerite and lamprophyre dykes; (4) sulfide veins of the NKT and Sopcha ore fields; (5) gabbro; melanonorite; and orthopyroxenite dykes; (6) gabbro-norite and anorthosite of the Monchetundra massif; (7) blastocataclasite after gabbroic rocks; (8) harzburgite and rocks of the NKT bottom zone; (9) alternation of harzburgites; olivine and olivine-free orthopyroxenes; (10) orthopyroxenite; (11) dunite, plagioclase-bearing dunite and chromitite of the Dunite Block; (12) ore layer 330 on Mt. Sopcha; (13) plagioclase-bearing orthopyroxenite; (14) melanonorite; (15) olivine norite and harzburgite; (16) rocks of Critical Unit at Mt. Nyud; (17) norite; (18) metagabbro-norite, gabbro, and anorthosite at foothills of Mt. Vurechuaivench; (19) amphibolized gabbro and (20) diorite of the 10th Anomaly; (21) silicic volcanics at Mt. Arvarench; (22) diorite and granodiorite, and (23) garnet-biotite, amphibole, and high-alumina gneisses and migmatites of the Archean complexes, and (24) faults.

The Monchepluton has an arched shape in plan close to its initial shape and consists of two chambers. One of them is 7 km long, oriented northeastward and expressed in Mts. Nittis, Kumuzh'ya and Travyanaya (hereinafter referred to as the NKT). The other 9 km long chamber stretches eastward from the top of Mt. Sopchuaivench to Mts. Nyuduaivench and Poazuaivench (hereinafter referred to as Sopcha, Nyud and Poaz) (Figure 2).

Up the sequence of the Monchepluton layered series, a regular transfer from ultramafic to mafic rocks occurs at differentiation crystallization (Figure 3). Several zones were identified: (1) basal quartz-gabbro-norite, (2) peridotite (harzburgite), (3) peridotite-orthopyroxenite (harzburgite-orthopyroxenite), (4) dunite-peridotite, (5) orthopyroxenite, (6) norite, (7) norite-gabbro-norite and (8) gabbro-norite-anorthosite. The regular change in the composition from the ultramafic to mafic rocks in the vertical cross-section is disturbed in a number of cases, e.g., by the presence of a PGE-bearing 330 horizon reef among the Sopcha orthopyroxenites and a “critical” horizon within the olivine-bearing Nyud rocks [1].

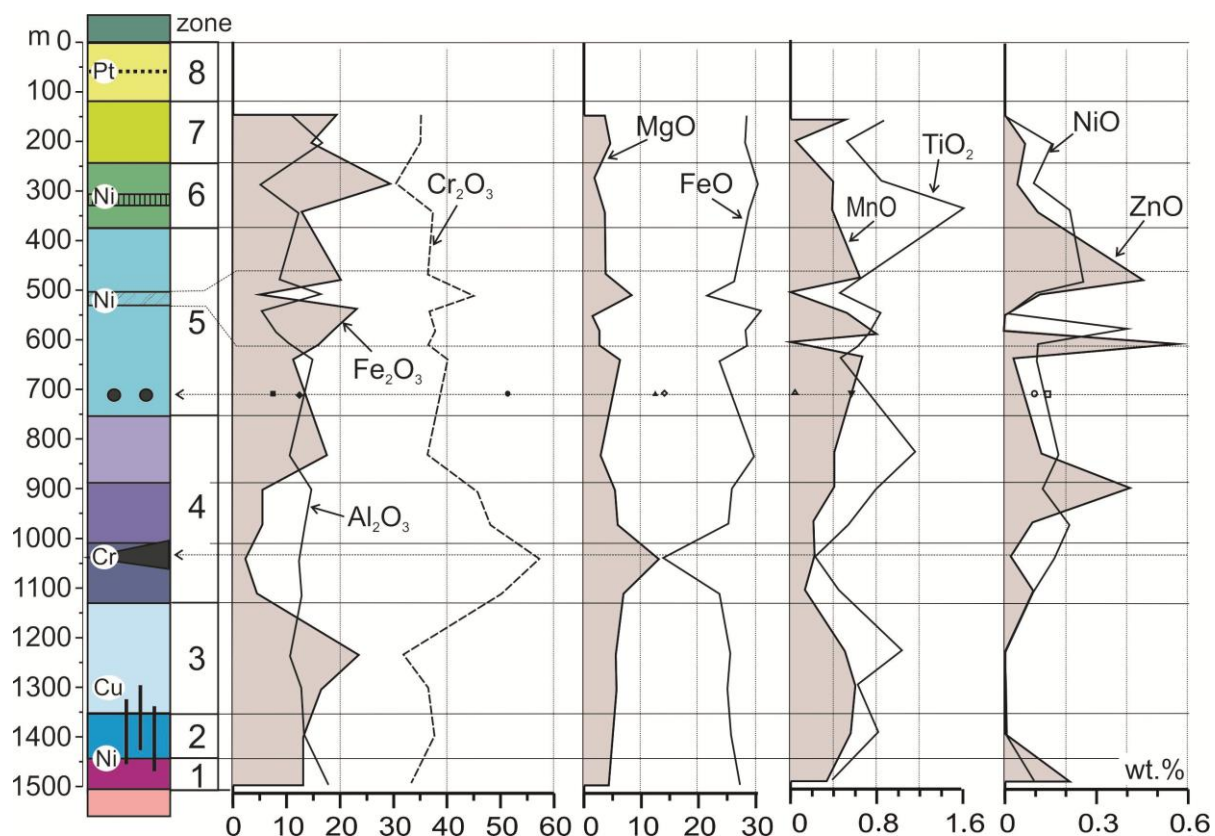


**Figure 3.** Variation of the Cr-spinel chemical composition of the Monchepluton layered series and Sopchezero deposit [2]. The colors are the same as those used in Figure 2.

The Monchepluton chromite deposit is confined to the southwestern part of the so-called Dunite Block. The chromitite layer is lens-shaped and constrained in the northeastern and southwestern parts by two main faults. The ore layer is about 1 km long and from 160 to 280 m wide. It dips southeastward with the maximum thickness of about 50 m. The northern part of the layer is obliterated by erosion.

The northeastern chamber (NKT and Sopcha massifs) is composed (from bottom to top) of quartz-bearing norites and gabbronorites of the basal zone with a thickness of 10–100 m, harzburgites (100–200 m), alternating harzburgites and orthopyroxenites (250–400 m), orthopyroxenites (300–700 m) with lenses of nodular chromitites (Kumuzh'ya) and layers of sulfide-bearing dunites-harzburgites with a thickness of 1–5 m (Sopcha, Ore Horizon 330). The total thickness of the NKT massif increases from north to south from 200–300 to 800–1000 m. The layered sequence in the Sopcha area is 1100–1600 m thick, which is the maximum for the Monchepluton.

The eastern chamber is composed of quartz-bearing gabbronorites and norites with a thickness of up to 50 m, melanocratic norites with lenses and interlayers of harzburgites and norites in the basal part. Its upper part comprises meso- and leucocratic norites and gabbronorites. The total thickness of the chamber cross-section varies from 300–400 m to 600–800 m. In the middle part of the Nyud cross-section, the so-called Critical Horizon occurs. It is rich in xenoliths of pyroxene-plagioclase and high-alumina hornfels and marks a transition from olivine-bearing to olivine-free, plagioclase-bearing rocks. The cross-section of the eastern chamber is completed by metamorphosed gabbronorites and anorthosites, which occur at the foot of Mt. Vurechuaivench. They are overlain by a micaceous weathering crust, conglomerates and Sumian volcanites.

A series of faults and thrusts breaks the Monchepluton into offset blocks. The largest faults (from west to east) within the NKT and the Mt. Sopcha are the Southern, the Latitudinal, the Northwestern, the Porphyry, the Meridional and the Northern faults.

Some of them, e.g., the Latitudinal, the Northwestern and the Porphyry faults, played the major role in formation of the NKT vein field and therefore control the distribution of ore veins. Three large faults (the Lamprophyry, the Central and the Eastern ones) divide the Nyud-Poaz massif into blocks. Geophysical data suggests that there is a large complex steeply-falling fault between the Mts. Nittis and Sopcha along Lake Sopch'yavr, which is confirmed by the recent drilling operations.

The Dunite Block containing the Sopchezero chromium deposit is located at the junction zone of the northeastern and eastern chambers of the Monchepluton (Figures 2 and 3). It has an irregular configuration and a complex internal structure due to the presence of a series of tectonic zones with a mainly northwestern strike and displacement amplitudes from a few meters to the first hundreds of meters. In the north and east, rocks of the Dunite Block contact ultramafic rocks of the Monchepluton, while in the southwest, they contact the main rocks of the Monchetundra massif. The contact is marked by a thick tectonic zone of garnet-amphibole blastocataclasites and a series of large dike-like bodies. According to drilling data, the vertical thickness of the Dunite Block varies from 100 to 700 m or more, increasing to the southeast. In the northeastern part, a significant part of the block was eroded and blocked by a moraine.

From southeast to northwest, dunite-peridotite, i.e., the host rock for the chromitites layer, is clearly altered in the composition. This variation is associated with increased orthopyroxene and plagioclase components. Dunite prevails in the southeastern part of the deposit, pyroxenite dunite dominates westwards and plagioclase-pyroxenite dunite prevails in the northwestern part. The secondary alteration represented by serpentinization of the olivine is attributed to tectonic faults.

Research data on many igneous deposits in the Urals and other regions show that the composition of accessory Cr-spinels with a varying composition and wide ranges of isomorphic substitutions that represent a continuous series of solid solutions from chromite to magnetite are well correlated with the composition of the host rocks [15]. Accessory Cr-spinels from harzburgite interlayers are distinct in a lesser content of  $\text{Fe}_2\text{O}_3$  and in a larger content of  $\text{Cr}_2\text{O}_3$ . In terms of other elements, they are close to and agree with the average composition of this zone differing in a high MgO and low  $\text{Al}_2\text{O}_3$  content. The contents of ZnO, NiO and  $\text{TiO}_2$  are low, while those of MnO are high. The dunite-harzburgite zone is represented by rocks of the Dunite Block composed of various rocks compositionally ranging from proper dunites to plagiodunites. In general, the rocks are characterized by high MgO and high  $\text{Cr}_2\text{O}_3$  composition at low contents of  $\text{Al}_2\text{O}_3$  and  $\text{FeO}_{\text{total}}$ . In addition, high NiO content is observed in the rock, especially in the harzburgites. With the transfer from dunites to harzburgites, the accessory Cr-spinels show reduced  $\text{Cr}_2\text{O}_3$  and increased  $\text{FeO}_{\text{total}}$  contents, but, in general, this zone is described by the Cr-spinels with highest  $\text{Cr}_2\text{O}_3$  and low  $\text{FeO}_{\text{total}}$  content.

In the Sopcha orthopyroxenite zone the  $\text{FeO}_{\text{total}}$  content continues increasing, whereas MgO, NiO and  $\text{TiO}_2$  decrease. The  $\text{Cr}_2\text{O}_3$  content in the rock significantly dropped at the transition from the dunite-harzburgite to the orthopyroxenite zone. The  $\text{Cr}_2\text{O}_3$  content in the Cr-spinels insignificantly diminished while the Sopcha pyroxenites contain higher  $\text{Cr}_2\text{O}_3$  and high MgO Cr-spinels compared to the Cr-spinels from the plagiodunites. The MnO content in the Cr-spinel continues growing at the abruptly reducing ZnO concentration.

With the transition to the norite zone composed by melanocratic norites, the  $\text{Cr}_2\text{O}_3$  and MgO content continues smoothly reducing, while the  $\text{FeO}_{\text{total}}$  concentration holds steady. The  $\text{Al}_2\text{O}_3$ ,  $\text{TiO}_2$  and  $\text{Na}_2\text{O} + \text{K}_2\text{O}$  content abruptly increases in the rock. The  $\text{Al}_2\text{O}_3$  content in the Cr-spinel insignificantly reduces. The  $\text{Cr}_2\text{O}_3$  content remains at the same level, while the  $\text{FeO}_{\text{total}}$  content mildly increases. An abrupt rise in the  $\text{TiO}_2$  content in the accessory Cr-spinels is highly sharp.

The norite-gabbro-norite zone composed by meso- and leucocratic norites and gabbro-norites shows an abrupt increase in the  $\text{Al}_2\text{O}_3$  and  $\text{Na}_2\text{O} + \text{K}_2\text{O}$  content, while the  $\text{Cr}_2\text{O}_3$  and NiO concentrations in these rocks are minimal. There are some variations in the  $\text{FeO}_{\text{total}}$  content, though, in general, the  $\text{FeO}_{\text{total}}$  content holds steady, while the MgO con-

tent keeps on dropping. The  $\text{Al}_2\text{O}_3$  content in the Cr-spinels also abruptly increases. The MgO content insignificantly increases at the expense of the reducing  $\text{FeO}_{\text{total}}$  concentration.

The regular changes in the composition of the accessory Cr-spinels in the layered series are disturbed within the PGE-bearing 330 horizon reef of Mt. Sopcha and “critical” horizon of Mt. Nyud (Figure 3). The PGE-bearing 330 horizon reef is inhomogeneous in terms of internal structure and composed of interrupted olivine and olivine-bearing rock layers. The changes in the accessory Cr-spinel composition along the layer cross-section are clearly irregular. The range of changes in the accessory Cr-spinel composition studied within the layer is just as wide as that for Cr-spinels from the rocks occurring in various parts of the Monchepluton stratigraphy, including those with an ultramafic and mafic composition. Such variations in the Cr-spinel composition in one thin layer represent an exception and are not observed in the other layered mafic-ultramafic intrusions of the Fennoscandian Shield, Stillwater and Bushveld complexes [1,2].

At the “critical” horizon within the transition zone from olivine norites to normal norites, there is an irregular alternation of meso- and melanocratic norites, plagiorthopyroxenites, gabbronorites, harzburgites, strongly hornfels high-alumina shists and bodies of micronorites and microgabbronorites. With the transition from the olivine-bearing to the olivine-free norites, the  $\text{FeO}_{\text{total}}$  content in the Cr-spinel increases twofold, norites of Mt. Nyud include accessory Cr-spinels with the highest  $\text{FeO}_{\text{total}}$  content at low  $\text{Cr}_2\text{O}_3$  and  $\text{Al}_2\text{O}_3$  concentrations (Figure 3).

## 2. Materials and Methods

Bulk data have been obtained by researchers from the Geological Institute KSC RAS supervised by Dr. Sci. (Geol.-mineral.) V.F. Smol'kin during their scientific investigations from 1998 to 2005 and onward. To study the structure of the ore deposit and the composition of chromite ores, the drill core was registered and tested, and oriented specimens were sampled in a prospecting quarry, where the photographic log of the ore objects was provided. The designation of boreholes with the ore intersections is shown in Figure 2.

The general data bank comprises 782 Cr-spinel analyses for the Monchepluton rocks, including 617 analyses for the Sopcheozero deposit [1,2] (Supplementary Materials, Table S1). The study of the mineral morphology, imaging in back-scattered electrons (BSEs) and preliminary chemical analyses were executed on polished sections with the use of the reflected light microscope Axioplan 2 Imaging (Karl Zeiss, Jena, Germany) and scanning electron microscope (SEM), LEO-1450 (Carl Zeiss, Oberkochen, Germany), with an energy dispersive X-ray analytical device (EDS) at the Laboratory of Physical Methods for Studying Rocks, Ores and Minerals of GI KSC RAS (Apatity, Russia). The chemical composition of minerals was measured in the MS-46 Cameca electron microprobe analyzer (EPMA) operating in WDS-mode. Accelerating voltage 22 kV, current strength of probe 30–40 nA. The beam size was 2–10  $\mu\text{m}$ , depending on stability of the matter under the beam current. The measurement time was 10 s for major elements, 20 s for minor elements, and 10 s for background measurements. The results of 4–5 measurements for each element were averaged. The microprobe analysis was performed for grains larger than 20  $\mu\text{m}$ . The used standards and limits of accuracy for each of the measured elements are shown in Table S2 (Supplementary Materials).

All Cr-spinel analyses were recalculated for formula values and basic coefficients applied to construct classification and variation diagrams [16].  $\text{FeO}_{\text{total}}$  was recalculated for formula values of  $\text{Fe}^{2+}$  and  $\text{Fe}^{3+}$  according to the stoichiometric formulae calculated based on the charge balance for O = 4 atoms per formula unit (a.p.f.u.).

Some studies of microinclusions in minerals and plastic deformations in olivine [17] were provided at the National Centre for Scientific Research CRPG-CNRS (Nancy, France) and the Jagiellonian University (Cracow, Poland).

Crystallization paleotemperatures of rocks and ores can be estimated using the coefficient of Mg and Fe distribution between coexisting Cr-spinel and olivine. This system is studied in detail in layered intrusions, dikes, volcanites and experimental systems with

the mafic melt under varied conditions [15,18–24]. For our analysis, we picked grains of accessory and ore Cr-spinels included in olivine or intergrown with it [1,2,25]. These Cr-spinels occur as euhedral to subhedral grains devoid of an optical zonation. Textural evidence arguing to olivine–Cr-spinel co-crystallization in the magmatic stage (e.g., the presence of olivine inclusions in Cr-spinel) is observed in all types of chromitite ores. Pairs of Cr-spinel-olivine from banded and massive rich ores, from supra-ore and sub-ore dunites were analyzed [1,2,25] (Supplementary Materials, Table S2).

We chose an advanced geothermometer which was developed based on experimental data on the Cr-spinel crystallization in typical MORB basalts [24]. The algorithm of Poustovetov and Roeder [24] allows estimating the spinel-melt equilibrium temperature and the composition of spinels. The studied spinel is presumed to be in equilibrium with the melt of the given composition. Thus, once the composition of olivines and model melts is known and the oxygen fugacity is evaluated, we can calculate the partition coefficient of iron and magnesium between olivine and melt ( $K_{D_{Mg-Fe^{2+}}}$ ). Knowing its value, we can define whether there was an equilibrium between olivine with this composition and a melt and, if any, at what temperature. The primary equilibrium temperature was set, then the value of  $K_{D_{Mg-Fe^{2+}}}$  was calculated for olivine with step 1 °C. The calculated value was compared with the estimate based on available data on the chemical composition of olivine. When direct estimates of  $K_{D_{Mg-Fe^{2+}}}$  differed from the calculated values within  $\pm 0.007$ , the calculation was stopped, otherwise, the next iteration was provided. The pressure was taken equal for all estimates, since its impact on  $K_{D_{Mg-Fe^{2+}}}$  is minor.

Concentrations of petrogenic elements were estimated by atomic absorption spectrometer AAnalyst 400 (PerkinElmer Inc., Waltham, MA, USA) (wt.%) in the Laboratory for Chemical Analysis of GI KSC RAS (Apatity, Russia). The accuracy limits of the wet chemical analysis are given in Table S3 (Supplementary Materials).

### 3. Results and Observations

#### 3.1. Morphology and Structure of the Sopcheozero Chromite Deposit

The Sopcheozero deposit is a gently-dipping lenticular-stratified body with a length of up to 1100 m (Profiles 2 to 22) and a width of 160 m (Profile 5) to 260–280 m (Profiles 10, 11 and 14) extending southeastward at an angle of 140° (Figure 4). The ore-bearing structure was drilled to depths of 320 (C-1596) to 350 m (C-1598). Northwestward of Profile 5, the ore body wedges out and becomes exposed under loose moraine deposits with a weathering crust at the base, and completely disappears on Profile 1. The length of the ore deposit's head part extending under the moraine is 190 m. The deposit is gradually sinking southeastward; on Profile 11, the ore layer is penetrated already at a depth of 150–200 m, and of 190–280 m and 280–310 m from the surface on Profile 14 and 22, respectively. The vertical thickness of the ore deposit in its head part (Profiles 3–6) varies from 3 to 10 m. With depth (southeastward), its thickness gradually increases to 15–18 m. Its maximum thickness reaches 30–34 m (Profile 14) and, less frequently, almost 50 m (Profile 20).

Pursuant to the analysis of fault tectonics, there are two main faults that constrain the ore deposit. They occur as blocking second-order feathering faults and polygonal cracks in the ore-bearing dunites. They form a single system of disjunctive dislocations, which formation time preceded the emplacement of gabbroids. A later system of fractures with a submeridional strike contains a regional complex of ferrodolerite-ferropicrite dikes. It makes no significant impact on the structure of the deposit, since the dikes are mainly represented by tension cracks. The main faults extending along the azimuth of 320–340° northwestern dip northeastward at an angle of 45–50°. A dike complex of microgabbro-microgranite that constrains the ore body from the northeast, intruded along one of them. It is a typical thrust along which the northeastern wing of the deposit was uplifted and eroded. The second fault of a normal type presumably constrains the ore deposit in the southwest, where dunites contact the rocks of the Monchepluton rhythmic series (boreholes 1524 and 1651) or coarse-grained gabbroids (boreholes 1523 and 1518).

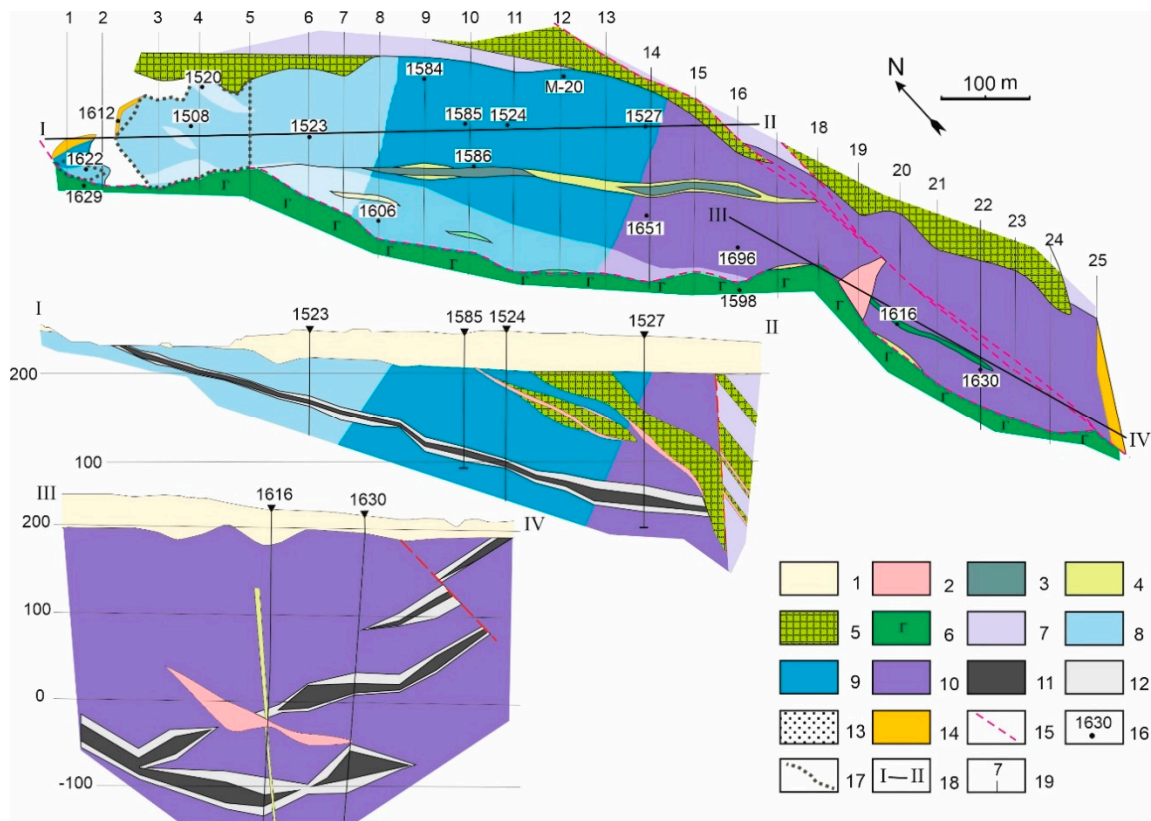


**Figure 4.** Geological map of the Sopchezero deposit and longitudinal sections [1,2]. (1) Moraine; (2) microgranite vein; (3) orthopyroxenite and norite dykes; (4) dyke of coarse-grained norite; (5) microgabbro and microdiorite dykes; (6) gabbroanorthosite of the Monchetundra massif; (7) barren and (8–10) ore-bearing ultramafic rock of the Dunite Block: (8) plagioharzburgite, (9) plagiodunite, (10) dunites; (11) rich and ordinary chromitite ores; (12) poor chromitite ore; (13) serpentinized ultramafic rocks; (14) rocks overlapped by a moraine; (15) faults; (16) borehole position and its number; (17) contour of an open pit; (18) geological section and its number; (19) exploration profile and its number.

Along the main and feathering faults, gabbroid dikes intruded. Numerous dikes of coarse-grained gabbroids breaking ore bodies through have a steep dip (up to vertical) and a predominantly northwestward strike. Subparallel microgabbro and microgranite dikes beyond the northeastern boundary of the deposit dip northeastward at an angle of 45–50°.

The study of the Cr-spinel mineralization showed no clear distribution of Cr-spinel at the deposit. The Cr-spinel content varies in a wide range from rich ores (>90%) to barren rocks (<2–3%), almost gradually, which makes it difficult to identify marker layers. The lower boundary of mineralized rocks (or chromitites) is determined by the minimum visually detectable Cr-spinel content of about 5% (at a Cr<sub>2</sub>O<sub>3</sub> content of at least 0.25%).

The internal structure of the ore body (Figure 5A) is characterized by lenticular stratification due to the vertical alternation of rich and ordinary (or poor) ores and absent correlation of its cross-sections even in the boreholes drilled in contiguous cross-sections. In certain intersections of ore layers, there are from 2–3 ore layers to 7 rich-ore layers and 11 ordinary-ore layers. The location of the rich-ore layers in the cross-sections and their thickness varies greatly from one cross-section to another. The orientation of the layer boundaries and the ore body as a whole is subparallel. Meanwhile, field measurements in the Sopchezero quarry performed by the authors in 2001 during the selection of oriented samples indicated a more gentle dipping in the ore banding (6–10°) compared to the general slope of the ore deposit (20–25°).

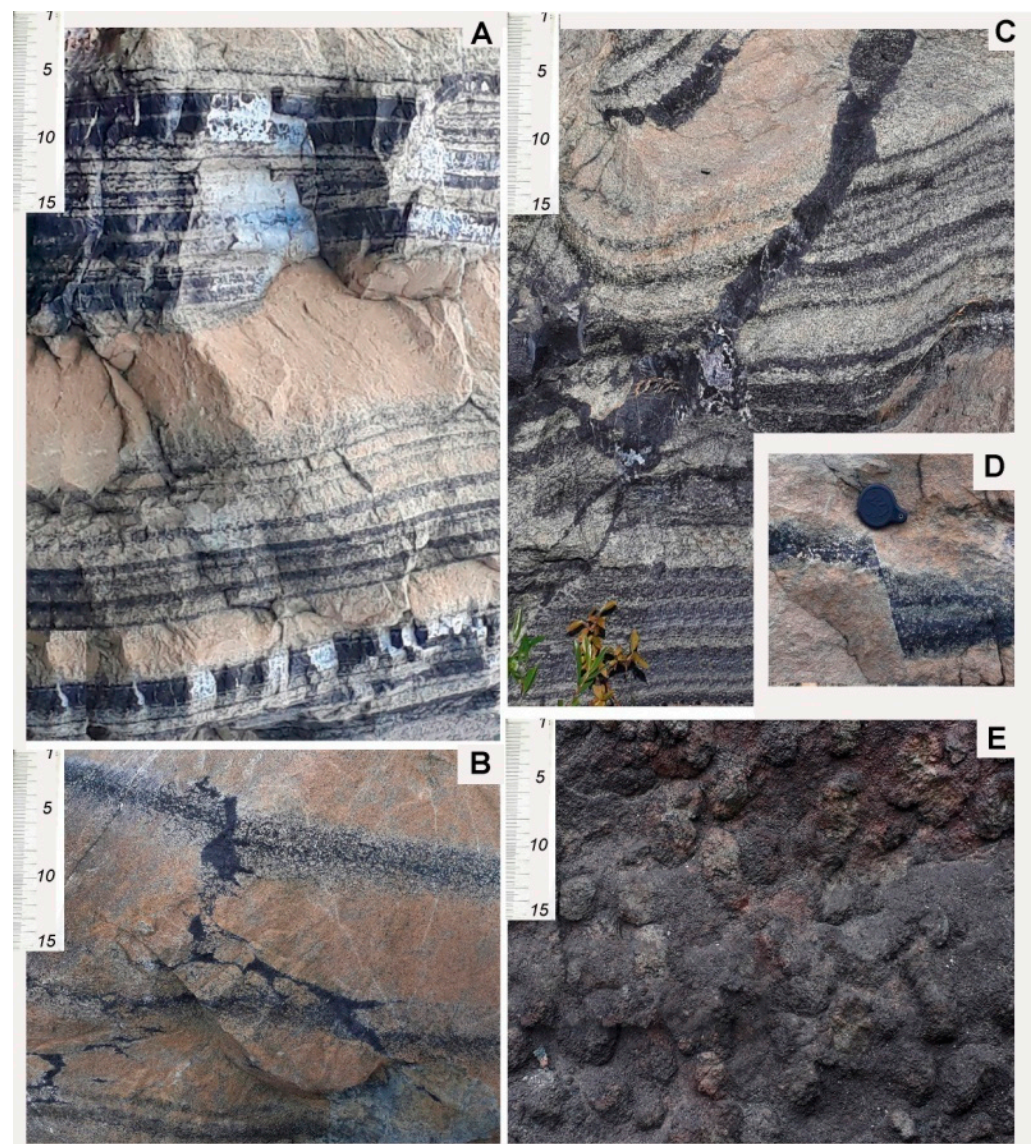


**Figure 5.** Features of the internal structure of the chromitite layers of the Sopcheozero deposit: (A) Alternation of rhythmically layered ore layers with host dunites; (B) Early segregations of ore matter in micro-fractures in ore layers with a cumulative structure; (C) Thin ore vein extending from the ore layer to the top along a diagonal crack in dunite; (D) Micro-displacement of the ore layer with massive and sideronite textures; (E) Nodular Cr-spinel of Mt. Kumuzhiya. Dimensions on the ruler are in cm.

Ore layers comprise thin injected ore veins that do not overstep the boundaries of the ore deposit (Figure 5B,C). Rocks and ores of the deposit are intersected by dikes with the basic composition and the age close to that of the Monchepluton rocks [1].

### 3.2. Zoning of the Dunite Block and Ore Body

For the Dunite Block, a clearly defined zoning is established: moving northwestward, the dunites at a depth are replaced by plagioclases overlain by plagioclase varieties sharply predominate with gradual transitions between the rocks. Mafic rocks (olivine norites and troctolites) are subordinate and form indistinctly expressed areas or segregations. Near the zones of tectonic disturbances, rocks undergo local serpentinization and chloritization.

The change in the dunite-peridotite composition associates with a gradual increase in their orthopyroxene and plagioclase content. The southeastern part of the deposit is dominated by proper dunitites, which are mainly poorly altered. Pyroxene dunitites represent the leading rock type in the central part of the deposit (between Profiles 7 and 13), less frequently found in its northwestern part, where the content of orthopyroxene and plagioclase in the rocks clearly increases at an uneven distribution that leads to an increase in the diversity of rocks from plagioclase-orthopyroxene varieties of dunite to plagioclase-harzburgite, harrisite (metatroctolite) and olivine melanonorite. Harzburgites relatively enriched in orthopyroxene form indistinctly expressed bodies in pyroxene-plagioclase dunitites, and those depleted in orthopyroxene associate with substantially plagioclase rocks such as troctolites and norites. For all the above-described rocks, the same order of crystallization of the mineral phases is established, i.e., Cr-spinel-olivine-orthopyroxene-(clinopyroxene)-plagioclase.

The zoning of dunite-peridotite is confirmed by their chemical compositions. Thus, the average CaO and Al<sub>2</sub>O<sub>3</sub> content in dunitites east of Profile 10 is 0.38 wt.% and 1.9 wt.%, while that between Profiles 8 and 4 and west of Profile 4 is 1.07 wt.% and 2.3 wt.% and 1.84 wt.% and 2.98 wt.%, respectively.

To investigate the relationship between the lateral zoning of the ore deposit and Cr-spinel composition, we studied Cr-spinels from the ore intersections of some boreholes. Figure 6 shows points that indicate an average content of the main components in Cr-spinels and lines of lateral change trends in the Cr-spinel composition along the ore deposit. Based on the analysis of the above diagrams, the following pattern is revealed: with the transition from plagioclase-harzburgites, plagioclase-dunitites to dunitites (Profiles 2 to 22), the content of Cr<sup>3+</sup> significantly increases and that of Al<sup>3+</sup> decreases. The Cr-spinels of the ore deposit are characterized by a low and relatively stable Fe<sup>3+</sup> content with a slight decrease in its content in the Cr-spinel from the northwest to the southeast as the ore deposit dips. Significantly ranging changes in the content of divalent elements (Fe<sup>2+</sup> and Mg<sup>2+</sup>) have been revealed to be probably resulted from the redistribution of these elements between Cr-spinel and olivine. The widest variations in the Fe<sup>2+</sup> and Mg<sup>2+</sup> contents are observed for plagioclase-dunitites and plagioclase-harzburgites (Profiles 8–10 and 14).

Thus, with an increase in the orthopyroxene and plagioclase content in the host ultramafic rocks, the ratio of the main components in Cr-spinel drastically changes since they are already redistributed between a large number of phases such as Cr-spinel, olivine, orthopyroxene, and partly, plagioclase.

It was initially assumed that the composition of ore Cr-spinel may vary in the cross-section of a particular ore body. To confirm this thesis, we studied the composition of Cr-spinel phases in the cross-section of ore intervals in boreholes 1520, 1527 and 1585, cutting various sectors of the ore body through (Supplementary Materials, Table S1; Figure 7A–C). The Cr<sup>3+</sup> content in ore Cr-spinels and the Cr# ratio varies within fairly narrow limits. The Mg# ratio changes more significantly and is zonal in nature; in the roof and basement, this ratio in the ore Cr-spinels is considerably lower than that in the main part of the ore body.

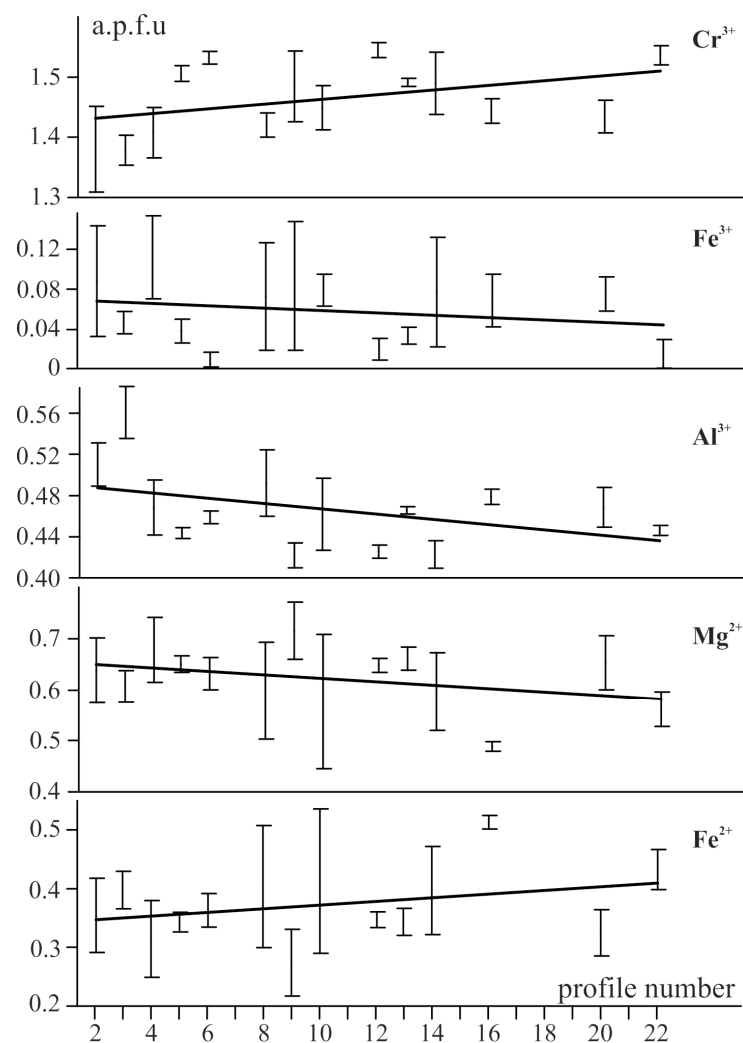


**Figure 6.** Relationship between the lateral zoning of the ore deposit and Cr-spinel composition. Designations of the profile numbers are shown in Figure 4.

It was found that, at the boundary of the ore body, in underlying and overlying rocks, accessory Cr-spinel is replaced at the edges by ferrochromite with Cr, Mg and Al removal that disturbs the above-noted zoning (Figure 7C). To a much lesser extent, substitution is manifested in ore Cr-spinel.

The above diagram shows that the Cr-spinel compositions regularly vary across the rock sequence, but they change most strongly within the ore body. The following pattern is established for accessory Cr-spinel: approaching the ore body, ratios of Mg# and Cr# increase. A similar trend is demonstrated by Cr-spinels from the underlying alternation zone, however, at a lower Cr<sub>2</sub>O<sub>3</sub> and MgO content. Within the contact of the Cr-spinel-bearing dunites and underlying orthopyroxenites, the Cr<sub>2</sub>O<sub>3</sub> content in the Cr-spinel composition and Mg# and Cr# ratios decrease, but increase in harzburgites interbedding with orthopyroxenites. Thus, the Cr-spinel composition is clearly correlated with the composition of rocks or ores without significant disturbances in the contact zone. The olivine compositions in dunites and harzburgites are similar and correspond to a more magnesian variety than that in the orthopyroxenites. The maximum forsterite content in the olivine is found in the lower part of the ore body, which is typical of the entire Sopchezero deposit.

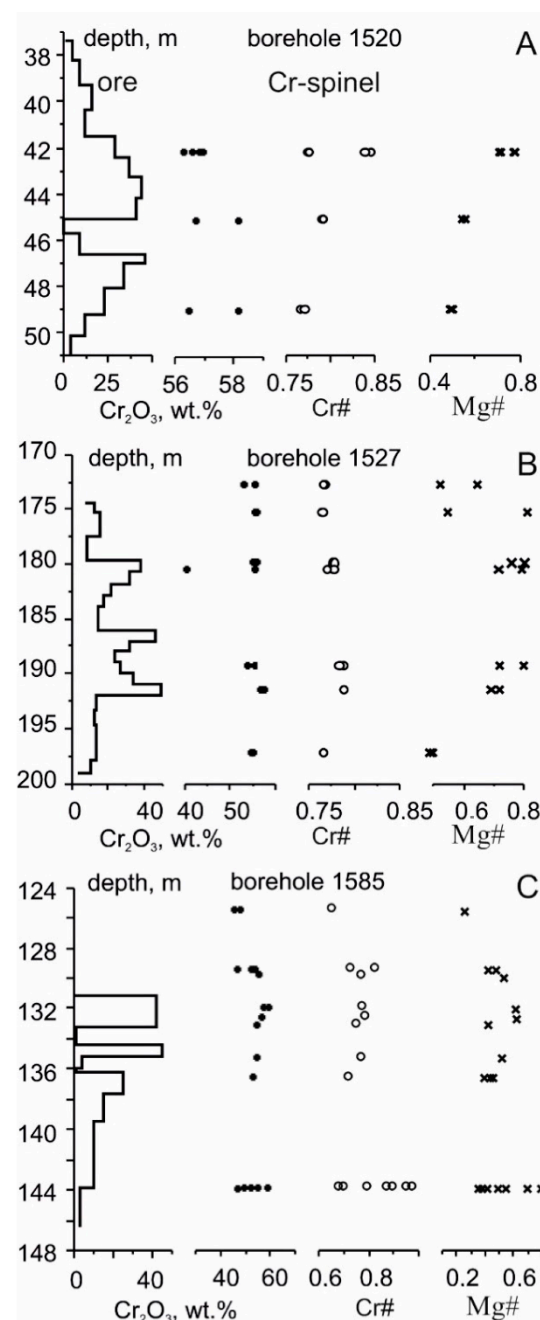


**Figure 7.** Composition of Cr-spinel phases in the cross-section of ore intervals in boreholes 1520 (A), 1527 (B), and 1585 (C). Indexes  $Cr\# = Cr/Cr + Al^{3+}$  and  $Mg\# = Mg/Mg + Fe^{2+}$  (a.p.f.u.). Designations of boreholes are shown in Figure 4.

### 3.3. Description of the Ore Composition of the Sopchezero Deposit

The ore composition is strongly dominated by Cr-spinel. The rock-forming minerals are represented by olivine, orthopyroxene, clinopyroxene, and plagioclase; the secondary minerals include serpentine, chlorite, actinolite, talc, clinocoisite, and carbonates. In addition to Cr-spinel, there is magnetite, titanomagnetite and ilmenite with minor pentlandite, heazlewoodite and native copper.

On the basis of studying the structural and textural features of the ores, Cr<sub>2</sub>O<sub>3</sub> content, content of the Cr-spinel and technological tests within the Sopchezero deposit, geologists from Severonickel and Geological and Mining Institute KSC RAS identified three ore types, i.e., the rich (thickly disseminated and massive), ordinary (thinly and thickly disseminated) and poor (disseminated and scattered) types [1,2].

The main industrial value are ores composed of magnochromite (50–65% Cr<sub>2</sub>O<sub>3</sub>), chrompicotite (35–55% Cr<sub>2</sub>O<sub>3</sub>) and alumochromite (35–50% Cr<sub>2</sub>O<sub>3</sub>). The most demanded and expensive raw materials for the metallurgical industry are ores with the Cr<sub>2</sub>O<sub>3</sub> content not less than 37–40 wt.% and the Cr<sub>2</sub>O<sub>3</sub>/FeO<sub>total</sub> > 2.5. These conditions are met only by magnochromite ores having a Cr<sub>2</sub>O<sub>3</sub>/FeO<sub>total</sub> > 3. The refractory and chemical industries use ores with a content of 32–35% Cr<sub>2</sub>O<sub>3</sub>, in which the Cr<sub>2</sub>O<sub>3</sub>/FeO<sub>total</sub> can be lower than 2 [26]. The Cr<sub>2</sub>O<sub>3</sub> average-weighted content in ordinary and rich ores of the Sopchezero deposit is 16.65 and 38.76 wt.%, respectively (Table 1), at gradually changing concentrations within the identified ore types and ore body in general. The ores of the Sopchezero deposit, having a ratio of Cr<sub>2</sub>O<sub>3</sub>/FeO<sub>total</sub> = 0.9–1.7, can serve as raw materials for the refractory and chemical industries.

**Table 1.** Average chemical composition of poor, ordinary and rich Cr-spinel ores of the Sopchezero deposit (wt.%) [1].

| wt. %        | Cr <sub>2</sub> O <sub>3</sub> | FeO   | Fe <sub>2</sub> O <sub>3</sub> | SiO <sub>2</sub> | CaO  | Al <sub>2</sub> O <sub>3</sub> | MgO   | P <sub>2</sub> O <sub>5</sub> | MnO  | TiO <sub>2</sub> |
|--------------|--------------------------------|-------|--------------------------------|------------------|------|--------------------------------|-------|-------------------------------|------|------------------|
| Rich ore     |                                |       |                                |                  |      |                                |       |                               |      |                  |
| n            | 140                            | 87    | 35                             | 111              | 107  | 81                             | 105   | 31                            | 28   | 26               |
| Max.         | 52.87                          | 16.0  | 15.53                          | 26.00            | 2.23 | 11.68                          | 30.58 | 0.02                          | 0.17 | 0.32             |
| Min.         | 30.11                          | 7.72  | 11.62                          | 7.00             | 0.10 | 5.89                           | 18.00 | 0.01                          | 0.09 | 0.16             |
| Avg.         | 38.76                          | 10.09 | 13.73                          | 13.70            | 0.56 | 8.96                           | 24.96 | 0.01                          | 0.13 | 0.21             |
| Ordinary ore |                                |       |                                |                  |      |                                |       |                               |      |                  |
| n            | 205                            | 102   | 35                             | 166              | 162  | 122                            | 160   | 43                            | 35   | 30               |
| Max.         | 29.72                          | 28.40 | 15.76                          | 39.00            | 6.38 | 17.88                          | 43.40 | 0.01                          | 0.18 | 0.29             |
| Min.         | 10.02                          | 5.66  | 8.94                           | 13.00            | 0.10 | 2.06                           | 11.00 | 0.00                          | 0.07 | 0.12             |
| Avg.         | 16.65                          | 8.90  | 10.55                          | 28.39            | 0.71 | 5.07                           | 34.39 | 0.01                          | 0.13 | 0.18             |
| Poor ore     |                                |       |                                |                  |      |                                |       |                               |      |                  |
| Max.         | 9.47                           | 10.19 | -                              | 42.05            | 1.26 | 3.51                           | 43.64 | 0.02                          | 0.13 | 0.18             |
| Min.         | 5.91                           | 6.51  | -                              | 20.00            | 0.52 | 1.88                           | 34.12 | 0.01                          | 0.10 | 0.08             |

Note. Samples from 37 boreholes. n—number of analyses, Max.—maximum, Min.—minimum and Avg.—average-weighted content. S content (wt.%): rich ore—0.078, ordinary ore—0.085, poor ore—0.1.

Rich ores contain more than 60% of Cr-spinel, which corresponds to the calculated Cr<sub>2</sub>O<sub>3</sub> content of >30 wt.%. These ores are characterized by a banded, spotted and massive texture, a medium-grained structure and a high-quality Cr-spinel. The average mineral phase contents (vol.%) are as follows: olivine—16, Cr-spinel—83, orthopyroxene <1, secondary minerals (serpentine, chlorite, talc, and amphibole)—15, and plagioclase <1.

Ordinary ores include mineralized ultramafic rocks with a Cr-spinel content of 20 to 60 vol.% that corresponds to the Cr<sub>2</sub>O<sub>3</sub> content varying from 10 to 30 wt.%. At the increasing Cr-spinel content, the scattered textures are replaced with thickly disseminated and banded ones with the simultaneous coarsening of the Cr-spinel aggregates. At the rising content up to 40 vol.%, Cr-spinel forms a continuous lattice with a cellular structure and sideronitic texture. The average mineral phase contents (vol.%) are to follow: olivine—58, Cr-spinel—29, ortho- and clinopyroxene—5, secondary minerals—8 and plagioclase <1.

Poor ore is characterized by a low Cr-spinel content which is less than 20 vol.% and corresponds to 10.6 wt.% of Cr<sub>2</sub>O<sub>3</sub>, and shows scattered distribution. They either alternate with ordinary ore or lie at the border of ore layers. The average mineral phase content (vol.%): olivine—66, Cr-spinel—10, ortho- and clinopyroxene—3, secondary minerals—21 and plagioclase <1.

Almost all ore types with rare exceptions are present in all cross-sections of the ore deposit, but the content and ratio between rich and ordinary ores vary significantly. Based on the analysis of ore intersections (73 boreholes) and at a cutoff grade for Cr<sub>2</sub>O<sub>3</sub> of 10 wt.%, rich ores make up 33%, ordinary ores—62.5%, poor ores—4.5% of the total deposit volume on the average.

Three groups of Cr-spinel grains are distinguished by their size [1]. Grain sizes of the main ore mass are mainly in the range of 0.05–1.2 mm. From low-grade to rich ones, there is an increase in the maximum grain size and average grain size of this Cr-spinel. The second group of Cr-spinel grains belongs to a fraction of 0.15–0.03 mm. They associate with the main phase of large Cr-spinel and olivine. In diagrams, this grain group creates a clear peak in all ore types. Finally, the third group of grains is represented by microinclusions of Cr-spinel in olivine and pyroxene with a size of less than 0.03 mm. They are also observed as a compact group in all ores, more frequently in poor ones and less frequently in rich ones.

Three main genetic types were identified based on the study of Cr-spinel morphology and its relationship with silicate minerals [1]. The first type is an early (pre-olivine or accessory) Cr-spinel that forms microinclusions in olivine. The second type is an ore Cr-spinel, which crystallizes simultaneously with olivine and somewhat later. The third type is a late Cr-spinel confined to interstices between olivine. In addition, there are late phases of Cr-spinel (in the form of inclusions in amphibole or confined to fractured zones) associated with its late redeposition, recrystallization and metamorphic transformations.

Accessory Cr-spinel occurs in host ultramafic rocks in the amount of first percents. Inclusions are represented by weakly faceted or oval grains with a prismatic habit up to 0.03–0.05 mm in size, mostly less than 0.01 mm. In a thin section, the grains have a rhombic or rectangular shape; the larger grains are usually rounded, possibly in result of resorption. The distribution of Cr-spinel inclusions in olivine is uneven and irregular. There are merely a few grains in the olivine section, but sometimes even a dozen. In certain areas, olivine is densely saturated with these Cr-spinel grains which make up max. 1% of the host-mineral volume. This Cr-spinel occurs in poor and ordinary ores as well as Cr-spinel-bearing rocks in small relics of olivine and replaced by serpentine.

Ore Cr-spinel represents the main type, which forms inclusions, nests, layers and veins of chromitite. The main mass of Cr-spinel in the ore layers shows grain sizes mainly in the range of 0.05–1.2 mm. The ores contain two morphological varieties of Cr-spinel with larger (>0.15–0.20 mm) and smaller grains (<0.20 mm). Both varieties show no zoning. The most fine-grained ores are found in the plagioperidotites and plagiodunites in the northwestern part of the deposit. The most coarse-grained ore occurs in dunites of its southeastern part. In the latter, the Cr-spinel size may reach 2.6 mm. The combination of coarse-grained and fine-grained Cr-spinel grains causes taxitic structures. In ores with an increased content of orthopyroxene and amphibole, idiomorphic Cr-spinel grains are also widely developed. They do not form solid aggregates, but are always separated by an intergranular silicate mass. In dunites-peridotites, Cr-spinel commonly occurs as grains between olivine grains, producing a sideronitic texture. Fine-grained Cr-spinel usually frames the coarser-grained one (Figure 8A) and is often included in the marginal parts of olivine.

Its position in the structure of the rocks implies that the main part of the ore Cr-spinel crystallized simultaneously with olivine, while the minor part formed upon the crystallization of olivine. The order of crystallization, morphology and composition within the ore deposit suggests the following generations are the early; the later, predominating and composing the main ore mass (ore Cr-spinel), and the late confined to interstices between olivine and orthopyroxene.

The early generation is a pre-olivine phase, like the accessory Cr-spinel in the country ultramafic rocks. It is observed as fine (0.005–0.05 mm) inclusions in olivine or less frequently in orthopyroxene in the amount of first percents. It mostly occurs in those ores that contain olivine and essentially represents a nonrecoverable phase in the applied technological process of ore dressing. The inclusions are primarily round-shaped, randomly distributed or less frequently oriented as a chain. During the serpentinization, the early generation is often preserved in olivine relics.

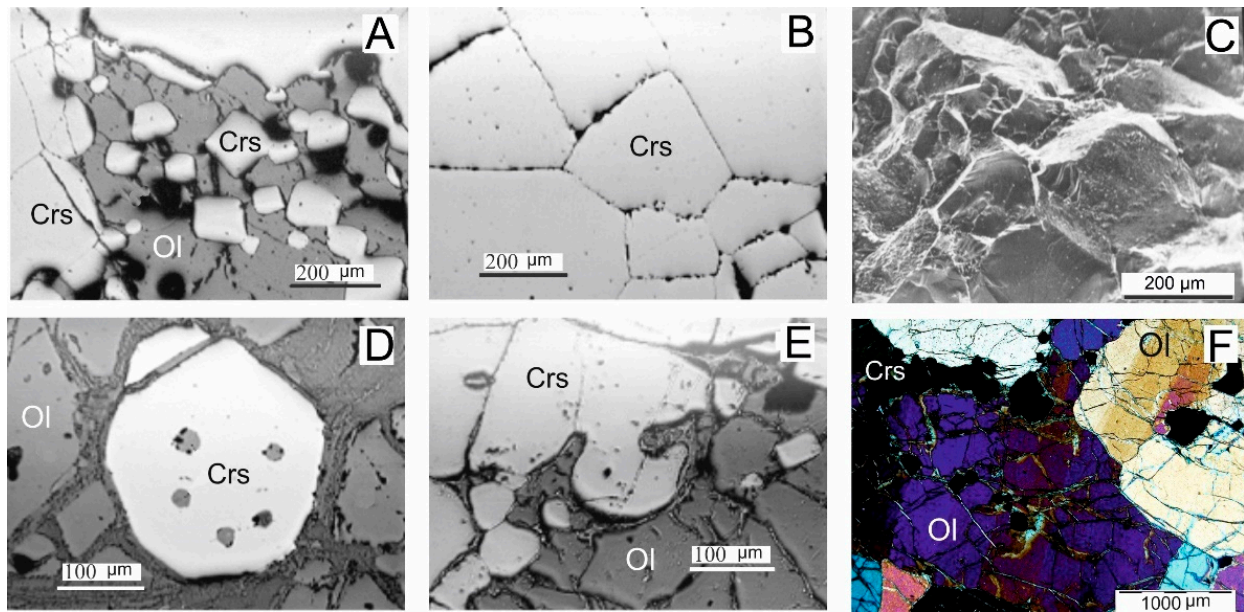


**Figure 8.** The morphological types of Cr-spinels and deformation of olivine from the Sopchezero deposit: (A) Fine-grained Cr-spinel (Crs) included in the olivine (Ol) marginal part (sample 1585/132.6); (B,C) Homogeneous Cr-spinel grains forming the densest package without inclusions of silicates (sample 1585/132.6); (D) The inclusions of olivine in Cr-spinel (sample 1598/33.6); (E) Idiomorphic combination of olivine and Cr-spinel (sample 1651/244.9); (F) Deformation of the olivine with polysynthetic twinning (sample 1651/201.4); (A,B,D,E) Back-scattered electron (BSE) images; (C) Secondary electron (SE) image; (F) Cross polarized light (CPL) image.

In the early generation, the content of  $\text{Al}_2\text{O}_3$ ,  $\text{FeO}$ ,  $\text{TiO}_2$  and  $\text{ZnO}$  decreases in contrast to the accessory Cr-spinel, but that of  $\text{MgO}$  and  $\text{Cr}_2\text{O}_3$  increases with the predominance of  $\text{Al}_2\text{O}_3$  over  $\text{MgO}$  (Table 2). Compositionally, it is likely an intermediate phase between accessory and ore Cr-spinel. An increased Ni content in the early generation indicates a low potential of sulfur during its crystallization.

**Table 2.** The average chemical composition of the Cr-spinel morphological types from the Sopchezero deposit (wt.%) [2,4].

| No.                                    | 1     | 2     | 3     | 4     | 5     | 6     | 7     | 8     |
|--|-------|-------|-------|-------|-------|-------|-------|-------|
| Chr-Type                               | I     | II    | III   | III-I | III-2 | III-3 | IV    | V     |
| n                                      | 8     | 2     | 66    | 3     | 26    | 1     | 2     | 337   |
| $\text{Cr}_2\text{O}_3$                | 42.21 | 50.10 | 55.39 | 55.92 | 56.07 | 54.87 | 55.01 | 51.13 |
| $\text{Al}_2\text{O}_3$                | 16.69 | 13.64 | 11.66 | 11.49 | 10.91 | 12.20 | 12.27 | 13.38 |
| $\text{TiO}_2$                         | 0.74  | 0.45  | 0.25  | 0.23  | 0.24  | 0.26  | 0.31  | 0.51  |
| $\text{FeO}_{\text{total}}$            | 31.31 | 21.61 | 16.04 | 18.95 | 16.14 | 15.74 | 20.41 | 22.36 |
| $\text{FeO}_{\text{calc.}}$            | 24.62 | 16.71 | 11.32 | 16.09 | 11.11 | 11.09 | 18.80 | 18.05 |
| $\text{Fe}_2\text{O}_3_{\text{calc.}}$ | 6.69  | 4.90  | 4.72  | 2.86  | 5.03  | 4.65  | 1.61  | 4.31  |
| $\text{MgO}$                           | 5.89  | 10.50 | 14.10 | 10.94 | 14.20 | 14.29 | 8.91  | 10.33 |
| $\text{MnO}$                           | 0.72  | 0.71  | 0.50  | 0.62  | 0.50  | 0.50  | 0.98  | 0.29  |
| $\text{NiO}$                           | 0.19  | 0.27  | 0.15  | 0.16  | 0.15  | 0.15  | 0.15  | -     |
| $\text{ZnO}$                           | 0.41  | 0.16  | 0.13  | -     | 0.07  | 0.14  | 0.22  | -     |
| $\text{CaO}$                           | 0.02  | 0.10  | 0.07  | -     | -     | 0.07  | 0.05  | -     |
| $\text{V}_2\text{O}_5$                 | -     | -     | -     | -     | -     | -     | -     | 0.13  |
| Total                                  | 98.18 | 97.54 | 98.29 | 98.31 | 98.28 | 98.22 | 98.31 | 98.13 |

Note: n—number of analyses. Chr-types I–IV [2]: I—accessory Cr-spinel from overlying and underlying ultramafic rocks; II—early generation in the form of inclusions in olivine; III—ore Cr-spinel, including: III-1—from sparsely disseminated, III-2—densely disseminated and III-3—sideronitic ores; IV—late generation; V—Cr-spinel from injection ore veins [4].

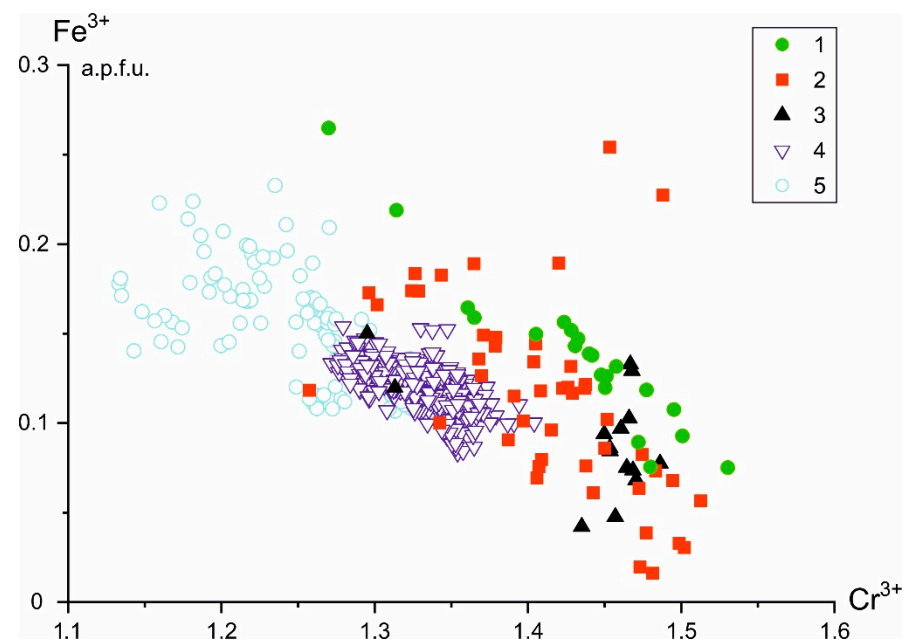
The ore Cr-spinel composes dissemination, layers, nests and less frequently injected vein-like bodies. The size of its grains varies widely from 0.05 to 2.6 mm, even in a single sample. The texture of the ore mass changes from disseminated, densely disseminated to sideronite, and homogeneous or massive. In the latter case, both allotriomorphic- and panidiomorphic-grained textures are observed. The panidiomorphic-grained texture is caused by the coalescence of relatively large, homogeneous grains of an octahedral (or hexagonal in the plane of the thin or thick sections) shape forming the densest package without inclusions of silicates (Figure 8B). The relationship between the ore and non-ore phases suggests that crystallization of ore Cr-spinel began together with olivine. However, its main mass was settled somewhat later than olivine, but before the crystallization of the orthopyroxene and plagioclase phases. This is evidenced by the inclusion of olivine in ore Cr-spinel (Figure 8C), and mutual, sometimes boxy, intergrowths of olivine and ore Cr-spinel, combination of equal idiomorphism of olivine and ore Cr-spinel and relative xenomorphism of ore Cr-spinel with respect to olivine (Figure 8D), as well as the extensive development of poikilitic inclusions of octahedral ore Cr-spinel in orthopyroxene. The microprobe analysis of the ore Cr-spinel-olivine pairs revealed them to be an equilibrium paragenesis.

Table 2 shows average compositions of ore Cr-spinel and also for ores separately, depending on their structural and textural features. The given data imply that ore Cr-spinel has the highest content of  $\text{Fe}_2\text{O}_3$  and  $\text{MgO}$ , which is accompanied by a decrease in the  $\text{Al}_2\text{O}_3$ ,  $\text{FeO}$ ,  $\text{TiO}_2$  and  $\text{ZnO}$  contents. It is characterized by both high and close concentrations of  $\text{MgO}$  and  $\text{Al}_2\text{O}_3$  with a constant predominance of  $\text{MgO}$  that distinguishes it from the early-generation or accessory Cr-spinel.

The late-generation Cr-spinel is observed as clearly anhedral grains or aggregates in the interstices between orthopyroxene or olivine. In terms of  $\text{Cr}_2\text{O}_3$  content, they are close to ore Cr-spinel differing in the increased  $\text{Al}_2\text{O}_3$  and  $\text{FeO}$  content and decreased  $\text{MgO}$  content (Table 2). This may be related to a low potential of the oxygen fugacity during the complete process of the ore melt crystallization. It is confirmed by the absence of late-magmatic Cr-spinel replacement with magnetite.

The secondary Cr-spinel related to the superimposed, locally developed dynamometamorphic processes confined to the zones of tectonic dislocations. It constantly associates with serpentine and chlorite and commonly occurs as a thin dissemination at the contact with olivine. Near the tectonic zones in the ores, there is a post-ore change in the primary Cr-spinel which is expressed in the appearance of intense fracturing in the ore Cr-spinel and the dissolution of the early Cr-spinel. The fracturing in Cr-spinel with a varied intensity is associated with serpentinization and the degree of its manifestation. Cr-spinel is often dissolved in blocks inside the crystal, while diffusive leaching is observed along cutting cracks and the periphery of grains. These areas show settling of small ilmenite grains in Cr-spinel, growth of magnetite and formation of light ferruginous phases on Cr-spinel. The manifestation of diffusive metasomatism on the periphery of Cr-spinel grains is most typical along with the formation of a shell of ferrochromite and magnetite in poor ores at Cr-spinel contents of less than 7 vol.%. In rich ores, Cr-spinel is almost never found undisturbed, especially at deep horizons, as it is broken up by parallel or reticulated cracks filled with secondary minerals.

Taking into account the most clearly manifested  $\text{Cr}^{3+}$ - $\text{Fe}^{3+}$  trend, a graph was constructed for the entire set of ore Cr-spinels depending on the type of ores and accessory Cr-spinels of the Dunite Block (Figure 9). Ore Cr-spinels on the graphs are clearly separated from the accessory type and are located in the field of the most chromic formations. The composition of Cr-spinel from injection veins clearly differs from the Cr-spinel from ore layers. It contains less  $\text{Cr}_2\text{O}_3$ , but more  $\text{MgO}$  and  $\text{Al}_2\text{O}_3$  with a close content of  $\text{FeO}_{\text{total}}$  (Table 2).



**Figure 9.** Binary variation diagram in terms of  $\text{Fe}^{3+}$  vs.  $\text{Cr}^{3+}$  (a.p.f.u.) showing the compositions of Cr-spinel from the (1) rich, (2) ordinary and (3) poor ores [1]; (4–5) Cr-spinel from the (4) injection ore veins and (5) host dunites [4].

### 3.4. Conditions of Cr-Spinel Origin

For analysis, we took non-zonal grains of accessory and ore Cr-spinel either included in olivine or intergrowing with it [1,2,25]. Ten coexisting Cr-spinel-olivine pairs from banded and massive rich ores, i.e., supra- and sub-ore dunites, were analyzed (Supplementary Materials, Table S2). Thermobarometric data reported here were obtained by the various authors using the equations of O’Neil–Wall–Ballhaus–Berry–Green (O’NWBBG) [22] and the algorithm of Poustovetov and Roeder [23,24] (Table 3).

**Table 3.** Model equilibrium temperatures of coexisting olivines and Cr-spinels from ores and host dunites of the Sopchezero deposit [1].

| N Sample       | Olivine |                  | Cr-Spinel |                  |      |      | $K_D \text{Mg-Fe}^{2+}$ | T, °C |                  |
|----------------|---------|------------------|-----------|------------------|------|------|-------------------------|-------|------------------|
|                | Mg      | $\text{Fe}^{2+}$ | Mg        | $\text{Fe}^{2+}$ | Cr   | Al   |                         |       | $\text{Fe}^{3+}$ |
| M33/1          | 0.97    | 0.03             | 0.81      | 0.19             | 0.66 | 0.23 | 0.11                    | 6.41  | 1258             |
| M33/2          | 0.97    | 0.03             | 0.81      | 0.19             | 0.64 | 0.23 | 0.13                    | 6.37  | 1258             |
| C-1616/343.4-1 | 0.93    | 0.07             | 0.62      | 0.38             | 0.74 | 0.23 | 0.03                    | 8.76  | 1225             |
| C-1616/343.4-2 | 0.93    | 0.07             | 0.60      | 0.40             | 0.75 | 0.23 | 0.02                    | 9.50  | 1225             |
| C-1612/12.2-1  | 0.89    | 0.11             | 0.52      | 0.48             | 0.66 | 0.27 | 0.08                    | 7.46  | 1179             |
| C-1612/12.2-3  | 0.88    | 0.12             | 0.54      | 0.46             | 0.67 | 0.27 | 0.06                    | 6.29  | 1169             |
| C-1612/9.8-1   | 0.87    | 0.13             | 0.30      | 0.70             | 0.56 | 0.33 | 0.11                    | 16.60 | 1163             |
| C-1612/9.8-3   | 0.87    | 0.13             | 0.31      | 0.69             | 0.57 | 0.32 | 0.10                    | 15.42 | 1164             |
| C-1612/16.1-3  | 0.87    | 0.13             | 0.33      | 0.67             | 0.59 | 0.33 | 0.08                    | 14.33 | 1163             |
| C-1612/16.1-4  | 0.87    | 0.13             | 0.37      | 0.63             | 0.58 | 0.32 | 0.10                    | 11.82 | 1165             |

Note: M33—banded rich ore; C-1612/12.2 and C-1616/343.4—rich ore; C-1612/9.8 and C-1612/16.1—supra-ore and sub-ore dunites.

Calculated temperature values range from 1258 to 1163 °C with the accuracy of  $\pm 50$  °C. Analysis of the obtained data indicates a clear trend, i.e., accessory Cr-spinels from sub- and supra-ore dunites show relatively lower temperatures compared to ore Cr-spinels from a deep-seated part of the ore deposit. Ore Cr-spinels also show varied temperature values, from high in the deep-seated part (C-1616/343.4) and low at lower depths (C-1612/12.2). However, this trend becomes broken in case of Cr-spinels from the quarry sample (M33). The latter are characterized by the maximum temperature of 1258 °C. As the temperature

and magnesium content in olivine decreases, redox settings change from reduced (QFM-1) in early cumulative horizons to QFM, QFM + 1 in dunites and QFM + 2 at the time of sideronitic texture formation [1].

The captured data comply with estimates of the crystallization paleotemperatures of intrusive rocks in the Monchepluton [25] obtained by orthopyroxene-clinopyroxene, clinopyroxene and orthopyroxene geothermometers [27]. The temperatures estimated using the O'NWBBG geothermometer [22] range from 600 to 700 °C. However, most of the temperatures obtained from the olivine-Cr-spinel equilibrium do not represent real liquidus temperatures. On the contrary, they reflect adjustment of the olivine-chromite Mg/Fe<sup>2+</sup> ratios in the post-magmatic stage and represent the closure temperature for the Mg-Fe<sup>2+</sup> exchange reaction.

Crucial data on the geological position of the Sopcheozero deposit in the Monchepluton structure and the inner structure of the ore deposit, the age of host and intersecting dike rocks, interrelations between different ore types with a varied useful component content, structural-textural features and a Cr-spinel composition in different generations are currently available to reconstruct the genesis of the Sopcheozero deposit. These data provide reliable interpretation of the Cr-spinel mineralization genesis as typical segregation and early magmatic that formed at the early stage of cooling and crystallization of the Cr-rich ore-silicate melt. Major crystallization and accumulation of ore Cr-spinel was temporally associated with the silicate phase, i.e., equilibrium high-magnesian olivine. Crystallization in the S-poor system under the low oxygen pressure provided intense enrichment of olivine in Ni ore layers. In addition to ore Cr-spinel, poor ores include an early phase of accessory Cr-spinel, while common and rich ores, though minor, contain a later interstitial phase. Disseminated and densely disseminated ores were formed by repeated rhythmic sedimentation of the ore and silicate phases. As for the massive ores, they might occur during the late magmatic recrystallization. In the results, admixtures were separated from ore Cr-spinel and a mosaic structure was produced. Crystallization temperatures of accessory and ore Cr-spinels differ. Thus, accessory Cr-spinels crystallized at lower temperatures compared to ore Cr-spinels. Cr-spinels are specifically marked by an increased content of Ti, which did not separate as an individual phase during subsolidus cooling, except for some cases, when ores were trapped by the basic melt of the dikes.

As the major melt finished crystallizing, host rocks and ores were subject to plastic deformations (Figure 8F). According to experimental data [17], it occurred under relatively high temperatures (above 400 °C) and general pressure (about 5 kbar), which provided a complicated inner structure of the deposit and, rarely, an intersecting bedding of banded and massive ores. Plastic deformations are clearly manifested in olivine and less markedly in orthopyroxenite and Cr-spinel. They are best observed at the contact between the ore deposit and host dunites, as well as in banded ores. As the Dunite Block became deformed, it was partly shifted as a hot wedge, which predetermined local brecciation of underlying rocks.

At the postmagmatic Svecofennian stage (1.84 Ga) [28], the primary geological position of the deposit was disturbed by tectonic shifts. They were caused by movement of blocks along the regional fault system separating the Monchepluton and Monchetundra massifs. It preconditioned local serpentinization, amphibolization, chloritization and, to a lesser extent, talcification of the silicate component, as well as reproduction of magnetite, ilmenite and sulfides.

In conclusion, we shall note that in terms of its geological structure, rock types and composition of ore Cr-spinels, the Sopcheozero deposit is closer to layered intrusions in East Karelia (Burakovskaya) and Finland (Kemi, etc.) than to the Ural deposits (Kempirsay, etc.) associated with ophiolitic complex [2].

## 4. Discussion

### 4.1. Problem of the Dunite Block Origin

The issue on the geological setting of the Cr-spinel-bearing Dunite Block in the Monchepluton composite cross-section has been long debated and discussed in literature. Many geologists [29–31] considered them as the earliest phase preceding the formation of major Monchepluton rocks based on the presence of dunite xenoliths in the underlying norites and orthopyroxenites. In this case, dunite with chromitite occurs as a lenticular body (or a plate) or a giant xenolith. However, this hypothesis was not confirmed, since it was established [1] that dunites were xenoliths not in intrusive rocks, but in mafic dike bodies. There is also no data on the intrusive relationship of the dunites with surrounding ultramafic rocks of the NKT or Mt. Sopcha.

According to the authors of [1], rocks of the Dunite Block are not xenoliths, an early or a late phase, but occur in the zone of rhythmically interbedding NKT orthopyroxenites and harzburgites (or of the northeastern chamber of the Monchepluton) as a regular member of the general Monchepluton cross-section. Their position was disturbed as a result of multiple post-intrusive tectonic movements. Rocks in the upper part of the cross-section are not known today. However, the lateral zoning associated with a transition from dunites to plagiodunites and plagioharzburgites suggests that overlying rocks may be represented by plagioclase-bearing ultramafic and, possibly, mafic rocks.

The generalized section along the M-20 borehole shows a complicated pattern [1]. Dunites occur at the surface and down to the depth of 388.5 m, all intersected by numerous veinlets of microgranites. Their continuity is often disturbed by small areas of intense shearing and mylonitization. An ore layer of rich banded ores mainly occurs at the depth of 158.3–171.6 m. A well-preserved primary contact between massive dunites (top) and underlying mottled porphyry harzburgites (bottom) is marked at the depth of 388.5 m, with harzburgites continuing to the depth of 399.6 m. In the interval of 399.6–923.5 m, a layered zone with interbedded orthopyroxenites and harzburgites occurs. Orthopyroxenites dominate in the section of this area, while harzburgites produce 0.4–2.0 m thick layers. The rocks are often brecciated and cemented by granophyre. The total amount of brecciated rocks is 25–30%. Down the section (int. 923.5–967.5 m), there are altered harzburgites and melanocratic mineralized norites with disseminated sulfides that contact host rocks, i.e., highly schistose and mylonitized biotite-amphibole gneisses intersected by highly schistose basic dikes (int. 967.5–983.7 m).

Thus, both boreholes intersected the lower contact of the Dunite Block rocks and got through most of the NKT massif section. One of them (borehole M-20) penetrated the underlying rocks of the Archean complex. In both cases, we observe weakly tectonically altered primary contacts between dunites and underlying orthopyroxenites, i.e., harzburgites. It allows concluding that rocks of the Dunite Block occur on a layered area or on a rhythmic interlayering zone of the Monchepluton NKT. Considering a set of their features, they cannot be an early phase, xenolith or a later phase intersecting the Monchepluton. New results of the U-Pb analysis of zircon [13] confirm that dunites and ores in the deposit have the same age with the Monchepluton rocks.

### 4.2. Ore Veins Issue

In 2016, a paper [4] based on the study of dump samples was published. One of the main conclusions was the presence of the podiform Cr-spinel mineralization in the Sopheozero deposit in the form of ore dikes intersecting ore layers.

Noteworthy, hypothetical ore dikes were not found in the quarry and boreholes intersecting the ore deposit, 57 in total. Ore dumps and the core of boreholes contained minor ore segregations and thin veins not exceeding ore layers (Figure 5B,C). They commonly start from the ore segregation in the frame of banded ores and continue upwards along vertical cracks. When veins branch, “microxenoliths” of host dunites and ores occur.

Analysis of the data [4] indicated that less than 5 cm thick veins have a relatively stable Cr-spinel composition, while veins with the thickness more than 5 cm show a clear

decrease in the MgO content and an increase in the  $\text{FeO}_{\text{total}}$  content from the central to the endocontact vein parts. It is caused by the decreased melting temperature in this direction. Vein Cr-spinel distinctly differ compositionally from Cr-spinel in ore layers. They are lower in  $\text{Cr}_2\text{O}_3$ , but higher in MgO and  $\text{Al}_2\text{O}_3$ , while the  $\text{FeO}_{\text{total}}$  is nearly the same (Table 2, Figure 9).

We believe that the vein type of the Cr-spinel mineralization was formed by primary segregation of the residual ore melt in ore layers, and then it was squeezed into supra-ore cracks. It provided isolation of the ore melt from bulk ore layers and crystallization of Cr-spinel with nearly no olivine. In the results, its MgO content increased. We can suggest that formation of the vein type of the Cr-spinel mineralization can be attributed to the above stage of plastic deformations of rocks and ores in the Dunite Block, i.e., up to the total cooling of the crystallized magma.

## 5. Conclusions

1. The Sopchezero deposit is a stratiform early-magmatic deposit typical of the Paleoproterozoic layered mafic-ultramafic intrusions of the Fennoscandian Shield.
2. The deposit occurs in the middle part of the dunite-peridotite zone, which is a member of the Monchepluton layered series. The U-Pb age of its formation ( $2500 \pm 10$  Ma) complies with the age limits of the whole pluton (2507–2496 Ma). Rocks and ores of the deposit are intersected by the same-age dikes of basic rocks. They intruded at the late stage of the Monchepluton evolution by filling contractional cracks by residual melts.
3. The deposit shows a clear lateral zonality regarding the composition of basic rocks. It is reflected in the increased content of intercumulus minerals, i.e., orthopyroxene and plagioclase in host rocks from the central part of the deposit to its flanks. It explains the transit from dunites to plagiodunites and plagiogabbros.
4. The deposit hosts rich, ordinary and poor ores that alternate in the section of ore layers. The  $\text{Cr}_2\text{O}_3$  content is >30, 10–30 and 10.6 wt.%, respectively. There are two zonality types of ore layers: normal, with rich ores occurring in the central part of the ore layer, and asymmetric, with rich ores in the lying flank. The ores are represented by rarely disseminated, disseminated, densely disseminated, sideronitic and massive types. Ore layers rarely comprise thin injection veins that do not produce a separate ore type. They can be referred to the podiform type, which is typical of deposits attributed to ophiolitic complexes.
5. The main ore phase is represented by magnochromite and magnoalumochromite with MgO slightly prevailing  $\text{Al}_2\text{O}_3$ , containing the admixture of Ti, Mn, V, Zn and Ni. Besides, the ores contain minor accessory and later interstitial phases. The ore phase is associated with highly magnesian olivine (96–98 Fo) rich in Ni (0.4–1.1 wt.%). It confirms a low S content in the melt and complies with the low oxygen fugacity.
6. The coexisting Cr-spinel-olivine pairs crystallized at temperatures from 1258 to 1163 °C, with accessory Cr-spinel crystallizing at relatively low temperatures, while ore Cr-spinel at higher temperatures.
7. Dunites and ores in the deposit distinguish with widespread plastic deformations of the translation gliding type in olivine, as well as in orthopyroxene and Cr-spinel at the postcrystallization phase under conditions of high temperature (above 400 °C) and general pressure (5 kbar). Plastic deformations are most common near and at the contact between dunites and ore layers, rarely right in layers.
8. At the postmagmatic Svecofennian stage (1.84 Ga) [28], the deposit jointly with the Monchepluton was subject to diverse tectonic deformations. In the results, it was divided into blocks. Some of them were destroyed by erosion. The tectonic deformations are also responsible for local alterations in rocks, i.e., serpentinization, chloritization, amphibolization and talcination, as well as replacement of the ore phase by magnetite.

**Supplementary Materials:** The following are available online at <https://www.mdpi.com/article/10.3390/min11070772/s1>. Table S1: Supplementary data with the average chemical composition of the Cr-spinels, Table S2: chemical composition of coexisting Cr-spinel-olivine pairs from the Sopchezero deposit. Table S3: The accuracy limits of the wet chemical analysis; the standards used and the analytical accuracy values of the EPMA.

**Author Contributions:** The authors have written the article together. A.V.M.: field works, maps and diagrams, investigations, interpretations; V.F.S.: field works, investigations, discussions, conclusions. Both authors have read and agreed to the published version of the manuscript.

**Funding:** The Geological Institute of the Kola Science Centre of Russian Academy of Sciences (GI KSC RAS 0226-2019-0053).

**Acknowledgments:** We are grateful to two anonymous reviewers and to members of the Editorial staff who helped us improve the presentation of our results. The authors express gratitude to staff of the Laboratory of Physical Methods for Studying Rocks, Ores and Minerals of the Geological Institute of the Kola Science Centre of the Russian Academy of Sciences (GI KSC RAS, Apatity, Russia); M. Ohnensteter and D. Ohnensteter (National Centre for Scientific Research CRPG-CNRS, Nancy, France); M. Huber (Maria Curie-Skłodowska University in Lublin, Poland). In addition, we would like to thank P. Yu. Plechov (Fersman Mineralogical Museum RAS, Lomonosov MSU, Moscow, Russia) for the assistance in the thermobarometric studies. The authors are also grateful to T.A. Miroshnichenko for the translation of the manuscript into English.

**Conflicts of Interest:** The authors declare no conflict of interest.

## References

- Smolkin, V.F.; Neradovsky, Y.N.; Fedotov, Z.A.; Dedyukhin, A.N.; Mokrushin, A.V. The Sopchezero chromite deposit confined to the Monchepluton. In *Layered Intrusions of the Monchegorsk Ore Region: Petrology, Mineralization, Isotopy, Deep Structure. Part 2*; Mitrofanov, F.P., Smolkin, V.F., Eds.; Geological Institute KSC RAS: Apatity, Russia, 2004; pp. 102–152. (In Russian)
- Mokrushin, A.V. Types, Composition and Conditions of Formation of Chromite Mineralization of Layered Early Proterozoic Intrusions of the Baltic Shield. Ph.D. Thesis, Murmansk State Technical University, Murmansk, Russia, February 2005; p. 155. (In Russian).
- Chashchin, V.V.; Galkin, A.S.; Ozeryanskii, V.V.; Dedyukhin, A.N. Sopchezero chromite deposit and its platinum potential, Monchegorsk pluton, Kola Peninsula (Russia). *Geol. Ore Depos.* **1999**, *41*, 460–468.
- Chistyakova, S.; Latypov, R.; Zaccarini, F. Chromitite dykes in the Monchegorsk layered intrusion, Russia: In situ crystallization from chromite-saturated magma flowing in conduits. *J. Petrol.* **2016**, *56*, 2395–2424. [[CrossRef](#)]
- Barkov, A.Y.; Martin, R.F.; Izokh, A.E.; Nikiforov, A.A.; Korolyuk, V.N. Ultramagnesian olivine in the Monchepluton (Fo96) and Pados-tundra (Fo93) layered intrusions (Kola peninsula). *Russ. Geol. Geophys.* **2021**, *62*, 324–338. [[CrossRef](#)]
- Smolkin, V.F. The Paleoproterozoic (2.5–1.7 Ga) midcontinent rift system of the northeastern Fennoscandian Shield. *Can. J. Earth Sci. Spes. Publ.* **1997**, *34*, 426–443. [[CrossRef](#)]
- Smolkin, V.F. Layered Intrusions of Early Proterozoic Basite-Ultramafic rocks of the Baltic Shield: Achievements and Problems. In *Petrology and Ore Content of the CIS and Baltic Shield Regions, Proceedings of the International (X All-Russian) Petrographic Meeting, Apatity, Russia, 20–22 June 2005*; KSC RAS: Apatity, Russia; pp. 251–253. (In Russian)
- Sharkov, E.V.; Chistyakov, A.V. Geological and petrological aspects of Ni-Cu-PGE mineralization in the early Paleoproterozoic Monchegorsk layered mafic-ultramafic complex, Kola Peninsula. *Geol. Ore Depos.* **2014**, *56*, 147–168. [[CrossRef](#)]
- Rundkvist, T.V.; Mokrushin, A.V.; Bazai, A.V.; Miroshnikova, Y.A.; Pripachkin, P.V. Xenolith of chromite-bearing dunites from the Sopcha massif (Monchegorsk complex, Kola Peninsula). *Notes Russ. Mineral. Soc.* **2011**, *3*, 99–109. (In Russian)
- Karykowski, B.T.; Maier, W.D.; Groshev, N.Y.; Barnes, S.-J.; Pripachkin, P.V.; McDonald, I. Origin of reef-style PGE mineralization in the paleoproterozoic Monchegorsk complex, Kola Region, Russia. *Econ. Geol.* **2018**, *113*, 1333–1358. [[CrossRef](#)]
- Amelin, Y.V.; Heaman, L.M.; Semenov, V.S. U-Pb geochronology of layered intrusions in the eastern Baltic Shield: Implication for timing and duration of Paleoproterozoic continental rifting. *Precambrian Res.* **1995**, *75*, 31–46. [[CrossRef](#)]
- Bayanova, T.; Mitrofanov, F.; Serov, P.; Nerovich, L.; Yekimova, N.; Nitkina, E.; Kamensky, I. Layered PGE Paleoproterozoic (LIP) intrusions in the N-E part of the Fennoscandian Shield—<sup>3</sup>He/<sup>4</sup>He data, summarizing U–Pb Ages (on baddeleyite and zircon), Sm–Nd data (on rock-forming and sulphide minerals), duration and mineralization. In *Geochronology—Methods and Case Studies*; Merner, N.A., Ed.; InTech: London, UK, 2014; Chapter 6; pp. 143–193.
- Chashchin, V.V.; Bayanova, T.B. Sopchezerskoye chrome deposit of Monchepluton: Geochemistry and U-Pb age. *Proc. Fersman Sci. Sess. Geol. Inst. KSC RAS* **2021**, *18*, 403–408. (In Russian)
- Smolkin, V.F. Kola–Norwegian province. *Early Proterozoic, In Early Precambrian of the Baltic Shield*; Glebovitskii, V.A., Ed.; Nauka: St. Petersburg, Russia, 2005; pp. 59–124. (In Russian)
- Barnes, S.J.; Roeder, P.L. The Range of Spinel Compositions in Terrestrial Mafic and Ultramafic Rocks. *J. Petrol.* **2001**, *42*, 2279–2302. [[CrossRef](#)]

16. Smolkin, V.F.; Mokrushin, A.V. Chrome-spinelides from layered intrusions of the paleoproterozoic Fennoscandian Shield as indicators of petro—and ore genesis. In *Springer Proceedings in Earth and Environmental Sciences*; Springer: Cham, Switzerland, 2021; in press.
17. Chernyshov, A.I. *Ultramafites (Plastic Flow, Structural and Petrostructural Heterogeneity)*; Charodey: Tomsk, Russia, 2001; p. 216. (In Russian)
18. Irvine, T.N. Chromian spinel as a petrogenetic indicator. Part I: Theory. *Can. J. Earth Sci.* **1965**, *2*, 648–672. [[CrossRef](#)]
19. Sack, R.O.; Ghiorso, M.S. Chromian spinels as petrogenetic indicators: Thermodynamics and petrological applications. *Am. Mineral.* **1991**, *76*, 827–847.
20. Roeder, P.L.; Reynolds, I. Crystallization of chromite and chromium solubility in basaltic melts. *J. Petrol.* **1991**, *32*, 909–934. [[CrossRef](#)]
21. Kamenetsky, V.S.; Crawford, A.J.; Meffre, S. Factors controlling chemistry of magmatic spinel: An empirical study of associated olivine, Cr-spinel and melt inclusions from primitive rocks. *J. Petrol.* **2001**, *42*, 655–671. [[CrossRef](#)]
22. Ballhaus, C.; Berry, R.F.; Green, D.H. High pressure experimental calibration of the olivine–orthopyroxene–spinel oxygen geobarometer: Implications for the oxidation state of the upper mantle. *Contrib. Mineral. Petrol.* **1991**, *107*, 27–40. [[CrossRef](#)]
23. Poustovetov, A.A.; Roeder, P.L. Numerical modeling of major element distribution between chromian spinel and basaltic melt, with application to chromian spinel in MORBs. *Contrib. Mineral. Petrol.* **2001**, *142*, 58–71. [[CrossRef](#)]
24. Poustovetov, A.A.; Roeder, P.L. The distribution of Cr between basaltic melt and chromian spinel as an oxygen geobarometer. *Can. Mineral.* **2001**, *39*, 309–317. [[CrossRef](#)]
25. Mokrushin, A.V.; Smolkin, V.F. Geothermobarometry of mafic-ultramafic rock of the Early Proterozoic stratified Monchapluton intrusion (Kola Peninsula). In *Geology and Geoecology: Studies of the Young, Proceedings of the XVI Conference of Young Scientists, Dedicated to the Memory Prof. K.O. Kratz, Apatity, Russia, 15 November 2005*; Mitrofanov, F.P., Ed.; KSC RAS: Apatity, Russia, 2005; pp. 282–285. (In Russian)
26. Smolkin, V.F.; Tkachev, A.V. Evolution of the metallogeny of chromite deposits through the Earth’s geological history. *NVNovit. News Vernadsky State Geol. Mus. Russ. Acad. Sciences. Dedic. 260th Anniv. Mus.* **2019**, *16*, 172–181. (In Russian)
27. Perchuk, L.L. Improvement of a two-pyroxene geothermometer for deep peridotites. *Dokl. USSR Acad. Sci.* **1977**, *233*, 456–459. (In Russian)
28. Sharkov, E.V.; Smolkin, V.F.; Belyatskii, V.B.; Chictyakov, A.V.; Fedotov, Z.A. Age of the Moncha Tundra fault, Kola Peninsula: Evidence from the Sm-Nd and Rb-Sr isotopic systematics of metamorphic assemblages. *Geochem. Int.* **2006**, *44*, 317–326. [[CrossRef](#)]
29. Kozlov, E.K. *Natural Rock Series of Nickel-Bearing Intrusions and Their Metallogeny*; Nauka: Leningrad, Russia, 1973; p. 288. (In Russian)
30. Dokuchayeva, V.S. Dunites from intrusions of the peridotite-gabbro-norite formation type in the Monchegorsk region. In *Basic-Ultrabasic Magmatism of the Kola Peninsula*; Gorbunov, G.I., Ed.; Kola branch of the USSR Academy of Sciences: Apatity, Russia, 1978; pp. 109–130. (In Russian)
31. Sushchenko, A.M.; Sidelnikov, M.V.; Groshev, N.Y. Petrography of xenoliths of chromite-bearing rocks from mount Kumuzhiya, Monchegorsk Complex, Russia. *Transact. Kola Sci. Cent. Russ. Acad. Sci. Geol. Geochem. Ser. 1* **2019**, *6*, 248–254. (In Russian)